Vietnam Journal of Mechanics, Vol. 48, No. 2 (2026), pp. 161 – 172
DOI: https://doi.org/10.15625/0866-7136/23630

FORMATION TRACKING OF MOBILE ROBOTS BASED ON LOCALLY MEASURED RELATIVE POSITIONS WITH VELOCITY SATURATION

Quoc Van Tran*, Ngoc-Bao Huu Tran, Quang-Hoang Nguyen
School of Mechanical Engineering, Hanoi University of Science and Technology, Hanoi, Vietnam
E-mail: quoc.tranvan@hust.edu.vn

Received: 16 October 2025 / Revised: 18 December 2025 / Accepted: 20 January 2026
Published online: 9 June 2026

Abstract. This work addresses the formation tracking of a team of multiple mobile robots subject to nonholonomic constraints and velocity saturation. A leader robot is used that follows a straight line with a constant speed. The other follower robots maintain the formation geometry by regulating the desired relative positions to neighboring robots. The measurement graph of the system is directed and contains a spanning tree rooted at the leader. Such a task is called formation tracking (or formation maneuvering in some works). The tracking controllers for the follower robots are designed to provide each robot's reference forward speed and angular rate, with their heading angles being estimated based on the robots' global positions. Asymptotic convergence to the target formation of the system is established. Simulation results and experimental results on formation tracking of mobile robots are provided to support the effectiveness of the proposed controller. A video of the experiment is provided in https://youtu.be/aKNtx02GNHQ.

Keywords: formation maneuvering, input saturation, multiagent systems, mobile robot, nonlinear stability analysis.

1. INTRODUCTION

Distributed control algorithms enable intelligent robotic systems to work cooperatively to complete a complex task using local onboard measurements. Many applications involving multi-robot systems, such as cooperative transportation, surveillance and exploration, require the robots to maneuver to different locations and maintain a certain geometry between them (i.e., a *formation*) (Ahn, 2019). One or more robots, called *leaders*, are aware of the formation path and can execute independent path-following controllers to track the reference trajectory (Cao & Tran, 2025). The other *follower* robots in the system are tasked with maintaining certain formation-induced inter-robot constraints, resulting in the maneuvering of the whole formation like a rigid body (L. Chen et al., 2023; Tran & Kim, Mar. 2022; Tran et al., 2023; Vu et al., 2024). In the literature, various constraints between the robots in the system have been utilized to specify the formation shape such as distances (J. Chen et al., 2024; Vu et al., 2024), directions (or bearing vectors) (Tran & Kim, Mar. 2022; Tran et al., 2023; Zhao & Zelazo, 2015), angles (L. Chen et al., 2023), and distance- and signed area-constraints (Kwon et al., 2022). The type of inter-robot constraints used often characterizes a certain number of such constraints and how they constrain pairs of robots so that the formation is unique (Ahn, 2019).

Early research studied formation tracking control schemes for point mass models (Ahn, 2019; L. Chen et al., 2022; Kwon et al., 2022; Vu et al., 2024). Formation tracking control protocols

were subsequently proposed for dynamical systems, for instance, wheeled vehicles (J. Chen et al., 2024; Tran & Kim, Mar. 2022), underactuated ships (Tran et al., 2023), and drone swarms (L. Chen et al., 2023; Schuck et al., 2025). Formation tracking of mobile robots has been investigated extensively in existing works (J. Chen et al., 2024; Khaledyan et al., 2020; Li et al., 2022; Lu et al., 2024; G. Sun et al., 2023; Z. Sun et al., 2019; Tran & Ahn, 2020; Tran et al., 2025; Tran & Kim, Mar. 2022). Formation tracking control of mobile agents based on orientation angle estimation that uses the relative orientations between the robots was addressed in Tran and Ahn (2020). The study (Tran & Kim, Mar. 2022) explored formation tracking controllers based solely on bearing vectors without the need for the leaders' velocity. A distance-based formation tracking control law for nonholonomic agents was presented in J. Chen et al. (2024) using the relative positions in local coordinates and the leaders' speed. The bearing-only formation maneuvering control method in Li et al. (2022) uses a consensus-based estimator for the follower robots to compute the leaders' time-varying velocity, thus requiring communication of the velocity estimates among the robots. Formation maneuvering control with velocity consensus was addressed in G. Sun et al. (2023) where each robot knows its neighbors' velocities. A distance-based formation maintenance scheme with a leader tracking a moving target was presented in Khaledyan et al. (2020). To obtain the formation velocity, similar to Li et al. (2022), the follower robots in the formation communicate the velocity estimates to neighboring robots. The study (Lu et al., 2024) proposed a relative position-based formation maneuvering controller employing barrier functions to ensure collision avoidance and connectivity maintenance between neighboring robots. The robots in the formation are aware of the formation velocity and have unconstrained control inputs. In the aforementioned studies, the control laws are designed as robots' reference velocities, which then can be easily converted to the wheels' desired speeds. Moving formation control with each agent moving in a distinct circle was investigated in Z. Sun et al. (2019). Each agent in the formation is provided with the desired heading speed and angular rate. For force-controlled mobile robots (Do, 2008; Maghenem et al., 2018), the control technique is employed to devise control forces to track the reference velocities. However, in Do (2008), the desired paths are given to the robots, making it a path tracking control protocol for each robot. The formation tracking controller in Maghenem et al. (2018) is restricted to systems with directed spanning tree graphs, i.e., each follower robot has precisely one direct leader and can obtain the leader's states via communication.

This article studies the formation tracking of multiple mobile robots based on the relative positions in the robots' respective local coordinates and under velocity input saturation. It is assumed that the heading angles of the robots are not available and are estimated from the global coordinates of the robots' positions via Yan et al. (2024). The contributions of this work are as follows. First, a formation tracking control scheme based on relative positions in local coordinates of the robots and orientation angle estimates is proposed. As opposed to L. Chen et al. (2022), Lu et al. (2024), G. Sun et al. (2023), and Z. Sun et al. (2019), the proposed controllers for the follower robots do not require the desired formation velocity nor the neighbors' velocities. Unlike Khaledyan et al. (2020), Li et al. (2022), and Maghenem et al. (2018), the robots are not required to estimate the leader's velocity, thus eliminating the communication burden in the system. Compared with Maghenem et al. (2018), the graph of the robots in this work is a general directed one that contains a spanning tree. Second, the formation is shown to converge to the target formation asymptotically even when the robots are subject to velocity saturation. In contrast, the tracking controllers in J. Chen et al. (2024), Khaledyan et al. (2020), Li et al. (2022), Lu et al. (2024), G. Sun et al. (2023), Z. Sun et al. (2019), Tran and Ahn (2020), Tran et al. (2025), and Tran and Kim (Mar. 2022) do not consider the effect of input limits. Finally, simulation results and experimental results on mobile Turtlebot3 robots are given to validate the theoretical analysis.

A preliminary version of this article was presented at the Fourth International Conference on Material, Machines, and Methods for Sustainable Development (MMMS2024) (Tran et al., 2025). Compared with Tran et al. (2025), the velocity limits of the robots are considered in this journal version. Furthermore, experimental results on formation maneuvering of mobile Turtle3 robots are provided in this article.

The remainder of this article is outlined as follows. Section 2 formulates the tracking control problem. The formation tracking controller is proposed and an asymptotic stability analysis is given in Section 3. Section 4 provides simulation results and Section 5 presents experimental results. Finally, Section 6 concludes this paper.

In this paper, we use boldface lowercase letters $\boldsymbol{x}, \boldsymbol{y}, \boldsymbol{z}$ to denote coordinate vectors and $\boldsymbol{X}, \boldsymbol{Y}, \boldsymbol{Z}$ to represent matrices. The stack vector of $\boldsymbol{x}_1, \ldots, \boldsymbol{x}_n$ is $\mathrm{vec}(\boldsymbol{x}_1, \ldots, \boldsymbol{x}_n) = [\boldsymbol{x}_1^\top, \ldots, \boldsymbol{x}_n^\top]^\top$. Denote by $\mathbb{R}$ and $\mathbb{R}^n$ the sets of real numbers and real n-dimensional vectors, respectively. Coordinate vectors expressed in the i-th local frame and the inertial coordinate frame are denoted with superscripts, e.g., $\boldsymbol{x}^{(i)}$, and without superscripts, e.g., $\boldsymbol{x}$.

2. PROBLEM DESCRIPTION

2.1. Multi-robot system

Consider a system of n mobile robots in the plane with each robot i ($i \in \mathcal{V} \triangleq \{1, \ldots, n\}$) having the position coordinates $\boldsymbol{p}_i \in \mathbb{R}^2$ and heading angle $\theta_i \in \mathbb{R}$ with regard to the inertial coordinate system $\mathcal{I}$ (see Fig. 1). The heading vector of robot i is $\boldsymbol{\xi}_i = \begin{bmatrix} \cos\theta_i \\ \sin\theta_i \end{bmatrix}$. Robot i's motion is governed by the kinematics:

$$\begin{aligned} \dot{\boldsymbol{p}}_i &= \boldsymbol{v}_i = u_i \boldsymbol{\xi}_i, \\ \dot{\boldsymbol{\xi}}_i &= \omega_i \begin{bmatrix} 0 & -1 \\ 1 & 0 \end{bmatrix} \boldsymbol{\xi}_i = \omega_i \boldsymbol{\eta}_i, \end{aligned} \tag{1}$$

where u_i is the heading speed, ω_i the angular velocity, and the lateral vector $\boldsymbol{\eta}_i = \begin{bmatrix} -\sin\theta_i \\ \cos\theta_i \end{bmatrix}$ of robot i (see the blue heading and lateral directions in Fig. 1). Notice that robot i can only move along the heading $\boldsymbol{\xi}_i$ according to (1), illustrating the nonholonomic motion constraint of the robot in the plane. The orientation of the robot can alternatively be described by the rotation

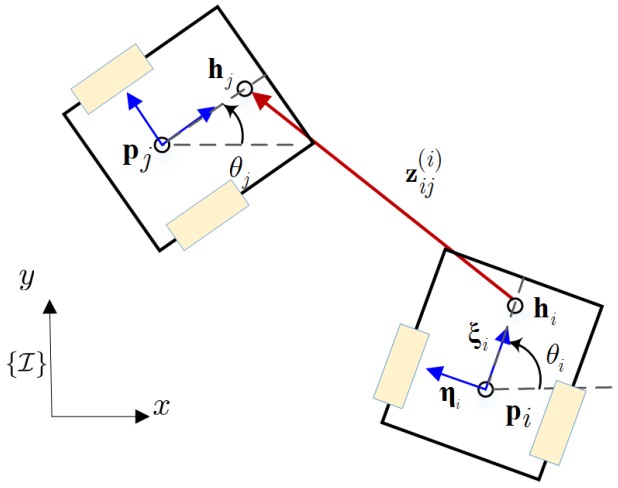

Fig. 1. The body-fixed coordinates $(\boldsymbol{\xi}_i, \boldsymbol{\eta}_i)$ of two-wheeled robot i. The relative position between the control points of robots i and j is $\boldsymbol{z}_{ij} = \boldsymbol{h}_j - \boldsymbol{h}_i \in \mathbb{R}^2$

matrix:

$$\boldsymbol{R}_i \triangleq [\boldsymbol{\xi}_i, \boldsymbol{\eta}_i] = \begin{bmatrix} \cos\theta_i & -\sin\theta_i \\ \sin\theta_i & \cos\theta_i \end{bmatrix} \in \mathbb{R}^{2\times 2}. \tag{2}$$

The global position $\boldsymbol{p}_i$ of the robot can be measured by an overhead camera or provided by the odometry data of the robot. In this work, however, the angle θ_i (thus, $\boldsymbol{R}_i$) is not measured; instead, it is estimated from the global position coordinates $\boldsymbol{p}_i$ of each robot i by an orientation observer (Yan et al., 2024):

$$\begin{aligned} \hat{\boldsymbol{\xi}}_i &= \boldsymbol{\chi}_i + k\boldsymbol{p}_i, \\ \dot{\boldsymbol{\chi}}_i &= \omega_i \begin{bmatrix} 0 & -1 \\ 1 & 0 \end{bmatrix} \hat{\boldsymbol{\xi}}_i - k u_i \hat{\boldsymbol{\xi}}_i,\ \boldsymbol{\chi}_i(0) = \boldsymbol{0}, \end{aligned} \tag{3}$$

where $\hat{\boldsymbol{\xi}}_i(t) \in \mathbb{R}^2$ is an estimate of the heading $\boldsymbol{\xi}_i(t)$ at time t, and $\boldsymbol{\chi}_i \in \mathbb{R}^2$ is an auxiliary integral vector of robot i. By using the observer (3) and assuming a positive heading speed, the estimate satisfies $\lim_{t\to\infty} \hat{\boldsymbol{\xi}}_i = \boldsymbol{\xi}_i$ exponentially fast. Note importantly that the estimate of the heading vector $\hat{\boldsymbol{\xi}}$ does not need to be a unit vector, even though one can easily normalize it.

In this work, we consider a *control point* $\boldsymbol{h}_i$ ahead of the $\boldsymbol{p}_i$ on the longitudinal direction $\boldsymbol{\xi}_i$ of each robot i with $\|\boldsymbol{h}_i - \boldsymbol{p}_i\| = L_i$. Thus $\boldsymbol{h}_i = \boldsymbol{p}_i + L_i\boldsymbol{\xi}_i$ and the control point's velocity:

$$\begin{aligned} \dot{\boldsymbol{h}}_i &= u_i\boldsymbol{\xi}_i + \omega_i L_i \boldsymbol{\eta}_i \\ &= [\boldsymbol{\xi}_i, L_i\boldsymbol{\eta}_i] \begin{bmatrix} u_i \\ \omega_i \end{bmatrix} \triangleq \boldsymbol{B}_i \begin{bmatrix} u_i \\ \omega_i \end{bmatrix}, \end{aligned} \tag{4}$$

where $\boldsymbol{B}_i = [\boldsymbol{\xi}_i, L_i\boldsymbol{\eta}_i] \in \mathbb{R}^{2\times 2}$ is an invertible input matrix. An estimate of the input matrix can be given as $\hat{\boldsymbol{B}}_i = [\hat{\boldsymbol{\xi}}_i, L_i\hat{\boldsymbol{\eta}}_i] \in \mathbb{R}^{2\times 2}$, where $\hat{\boldsymbol{\eta}}_i = \begin{bmatrix} 0 & -1 \\ 1 & 0 \end{bmatrix} \hat{\boldsymbol{\xi}}_i$. In the local coordinates of robot i, (4) can be written as

$$\boldsymbol{v}_{hi}^{(i)} = \boldsymbol{R}_i^\top(\theta_i)\dot{\boldsymbol{h}}_i = \begin{bmatrix} u_i \\ L_i\omega_i \end{bmatrix}. \tag{5}$$

2.2. Target formation and problem statement

The *target formation* $\boldsymbol{h}^* = \mathrm{vec}(\boldsymbol{h}_1^*, \boldsymbol{h}_2^*, \ldots, \boldsymbol{h}_n^*)$ of the system is specified by the motion of a leader robot, say, robot 1's trajectory $\boldsymbol{h}_1(t)$, and the desired *relative position* $\boldsymbol{z}_{ij}^* = \boldsymbol{h}_j^* - \boldsymbol{h}_i^*$ between pairs of neighboring robots i and j, as shown in Fig. 1. The leader is assumed to have a piece-wise constant velocity, i.e, v_c. These formation constraints can be depicted by relative positions over a *directed graph* $\mathcal{G} = (\mathcal{V}, \mathcal{E})$ with the edge set $\mathcal{E} \subseteq \mathcal{V} \times \mathcal{V}$. Here, if a directed edge $(i, j) \in \mathcal{E}$, robot i is aware of the desired relative position $\boldsymbol{z}_{ij}^*$ and measures the local displacement $\boldsymbol{z}_{ij}^{(i)} = (\boldsymbol{p}_j - \boldsymbol{p}_i)^{(i)}$ with regard to its local coordinates $(\boldsymbol{\xi}_i, \boldsymbol{\eta}_i)$ to robot j. The set of neighboring robots of robot i is $\mathcal{N}_i \triangleq \{j \in \mathcal{V} :\ (i, j) \in \mathcal{E}\}$. The *Laplacian matrix* $\mathcal{L} = [l_{ij}] \in \mathbb{R}^{n\times n}$ of the system is $l_{ij} = -1$ if $j \in \mathcal{N}_i$ $(j \neq i)$, $l_{ij} = 0$ if $j \notin \mathcal{N}_i$, and $l_{ii} = -\sum_{j\in\mathcal{N}_i} l_{ij}$. Denote $\boldsymbol{h}_F = \mathrm{vec}(\boldsymbol{h}_2, \ldots, \boldsymbol{h}_n)$ and the *system configuration* $\boldsymbol{h} = \mathrm{vec}(\boldsymbol{h}_1, \boldsymbol{h}_F)$.

We make the following assumption:

Assumption 1. *The graph of the formation $\mathcal{G}$ contains a spanning tree rooted at the leader. Each robot i measures local displacements $\boldsymbol{z}_{ij}^{(i)} = (\boldsymbol{p}_j - \boldsymbol{p}_i)^{(i)}$ in its local coordinates to neighbors $j \in \mathcal{N}_i$.*

Let $\boldsymbol{L} = (\mathcal{L} \otimes \boldsymbol{I}_2) \in \mathbb{R}^{2n\times 2n}$, where $\otimes$ is the Kronecker product. Arrange $\boldsymbol{L}$ into submatrices as follows

$$\boldsymbol{L} = \begin{bmatrix} \boldsymbol{L}_{ll} & \boldsymbol{L}_{lf} \\ \boldsymbol{L}_{fl} & \boldsymbol{L}_{ff} \end{bmatrix}, \boldsymbol{L}_{ll} \in \mathbb{R}^{2\times 2}, \boldsymbol{L}_{lf}, \boldsymbol{L}_{fl}^\top \in \mathbb{R}^{2\times 2(n-1)}, \boldsymbol{L}_{ff} \in \mathbb{R}^{2(n-1)\times 2(n-1)}.$$

$\boldsymbol{L}_{ff}$ is a diagonally dominant matrix that specifies the connections among the follower robots. Under Assumption 1, $\boldsymbol{L}_{ff}$ is invertible and contains positive eigenvalues, and the desired positions of the follower robots can be computed uniquely as Tran and Ahn (2020):

$$\boldsymbol{h}_F^*(t) = -\boldsymbol{L}_{ff}^{-1}\boldsymbol{L}_{fl}\boldsymbol{h}_1(t) + \boldsymbol{L}_{ff}^{-1}[\boldsymbol{L}_{fl}, L_{ff}]\boldsymbol{h}^*(t). \tag{6}$$

The leader is assumed to move at a piece-wise constant velocity $\boldsymbol{v}_c$. Note that the follower robots are unaware of the leader's velocity. The controller design is at the kinematic level, i.e., as reference velocity (u_i, ω_i) to the robots under the velocity saturation $|u_i| < u_{\max}$ and $|\omega_i| < \omega_{\max}$. The objective is to drive the follower robots to the target formation asymptotically, i.e., $\boldsymbol{\delta}_F = \boldsymbol{h}_F - \boldsymbol{h}_F^* \to \boldsymbol{0}$ as $t \to \infty$.

Based on this, the desired speeds of the motors in the actuated wheels can be straightforwardly computed. The low-level speed control in the robot's actuators can then track the reference speeds. As shown in the experiment section, the actual robots can arrive at the target formation by providing the designed velocity inputs.

3. FORMATION TRACKING CONTROLLER AND STABILITY ANALYSIS

This section proposes a formation tracking control law based on heading angle estimates and local displacements $\boldsymbol{z}_{ij}^{(i)}$. The convergence of the robots to the target formation subject to velocity saturation is established.

3.1. Formation tracking control protocol

The nominal tracking control law for each follower robot i is designed as follows:

$$[u_i^r, L_i\omega_i^r]^\top = k_P \sum_{j\in\mathcal{N}_i}(\boldsymbol{z}_{ij}^{(i)} - \hat{\boldsymbol{R}}_i^\top \boldsymbol{z}_{ij}^*) + k_I\hat{\boldsymbol{R}}_i^\top \int_0^t \sum_{j\in\mathcal{N}_i}(\hat{\boldsymbol{R}}_i\boldsymbol{z}_{ij}^{(i)}(\tau) - \boldsymbol{z}_{ij}^*)\mathrm{d}\tau \tag{7}$$

where $\hat{\boldsymbol{R}}_i = [\hat{\boldsymbol{\xi}}_i, \hat{\boldsymbol{\eta}}_i]$ is an estimate of the orientation matrix, and $k_P, k_I > 0$. The first term in the preceding controller is a formation stabilization term that minimizes the relative position errors on the edges. Since the follower robots do not have information on the leader's velocity $\boldsymbol{v}_c$, an integral action has been used in controller (7). The integral action, however, can only deal with unknown constant variables.

We define the saturation gains for the inputs in the preceding (7) as:

$$\begin{cases} s_{ui} = 1 & \text{if } |u_i^r| \le u_{\max} \\ s_{ui} = u_{\max}/|u_i^r| & \text{if } |u_i^r| > u_{\max} \end{cases}, \quad \begin{cases} s_{\omega i} = 1 & \text{if } |\omega_i| \le \omega_{\max} \\ s_{\omega i} = \omega_{\max}/|\omega_i| & \text{if } |\omega_i| > \omega_{\max} \end{cases} \tag{8}$$

Thus, the command velocity under saturations for robot i can be computed as:

$$\begin{aligned} \begin{bmatrix} u_i \\ \omega_i \end{bmatrix} = \begin{bmatrix} s_{ui}u_i^r \\ s_{\omega i}\omega_i^r \end{bmatrix} = \begin{bmatrix} s_{ui} & 0 \\ 0 & s_{\omega i}L_i^{-1} \end{bmatrix} \Big[& k_P \sum_{j\in\mathcal{N}_i}(\boldsymbol{z}_{ij}^{(i)} - \hat{\boldsymbol{R}}_i^\top \boldsymbol{z}_{ij}^*) \\ & + k_I\hat{\boldsymbol{R}}_i^\top \int_0^t \sum_{j\in\mathcal{N}_i}(\hat{\boldsymbol{R}}_i\boldsymbol{z}_{ij}^{(i)}(\tau) - \boldsymbol{z}_{ij}^*)\mathrm{d}\tau \Big]. \end{aligned} \tag{9}$$

In the presence of velocity saturation, the robots' control points are shown to be bounded in finite time.

Lemma 1. *Let Assumption 1 hold. Under the action of controller (9), the solution trajectory of the system* $\boldsymbol{h}(t) = \mathrm{vec}(\boldsymbol{h}_1, \ldots, \boldsymbol{h}_n)$ *does not have finite escape time.*

Proof. Since it is assumed for the leader $\boldsymbol{h}_1(t) = \boldsymbol{h}_1^*(t)$. By (5), one can see that the control point of follower robot i:

$$\begin{aligned}\|\boldsymbol{h}_i(t)\| &= \left\|\int_0^t \dot{\boldsymbol{h}}_i(\tau)\mathrm{d}\tau\right\| = \left\|\int_0^t \boldsymbol{R}_i \begin{bmatrix} u_i \\ L_i\omega_i \end{bmatrix} \mathrm{d}\tau\right\| \\ &\leq \int_0^t \|\boldsymbol{R}_i(\tau)\|\|[u_i, L_i\omega_i]^\top\|\mathrm{d}\tau \leq \int_0^t \sqrt{u_{\max}^2 + L_i^2\omega_{\max}^2}\mathrm{d}\tau \\ &\leq t\sqrt{u_{\max}^2 + L_i^2\omega_{\max}^2}, \forall i = 2, \ldots, n.\end{aligned}$$

This shows that $\boldsymbol{h}(t)$ does not blow up to infinity in finite time. □

3.2. Convergence analysis

Since the robots' orientation estimates $\lim_{t\to\infty} \hat{\boldsymbol{R}}_i = \boldsymbol{R}_i$ exponentially fast under (3) and the system configuration $\boldsymbol{h}(t)$ is bounded in time $t < \infty$, we consider that in the steady state, $\hat{\boldsymbol{R}}_i \approx \boldsymbol{R}_i$ in (9). To proceed, substituting controller (9) into (5) and using $\boldsymbol{R}_i\hat{\boldsymbol{R}}_i^\top = \boldsymbol{I}_2$ gives

$$\begin{aligned}\dot{\boldsymbol{h}}_i = \boldsymbol{R}_i \begin{bmatrix} u_i \\ L_i\omega_i \end{bmatrix} &= \begin{bmatrix} s_{ui} & 0 \\ 0 & s_{\omega i} \end{bmatrix} \Big[k_P \sum_{j\in\mathcal{N}_i} (\boldsymbol{z}_{ij} - \boldsymbol{R}_i\hat{\boldsymbol{R}}_i^\top \boldsymbol{z}_{ij}^*) \\ &\quad + k_I \boldsymbol{R}_i\hat{\boldsymbol{R}}_i^\top \int_0^t \sum_{j\in\mathcal{N}_i} (\hat{\boldsymbol{R}}_i\boldsymbol{R}_i^\top \boldsymbol{z}_{ij}(\tau) - \boldsymbol{z}_{ij}^*)\mathrm{d}\tau\Big] \\ &= \begin{bmatrix} s_{ui} & 0 \\ 0 & s_{\omega i} \end{bmatrix} \Big[k_P \sum_{j\in\mathcal{N}_i} (\boldsymbol{z}_{ij} - \boldsymbol{z}_{ij}^*) + k_I \int_0^t \sum_{j\in\mathcal{N}_i} (\boldsymbol{z}_{ij}(\tau) - \boldsymbol{z}_{ij}^*)\mathrm{d}\tau\Big].\end{aligned}$$

Let the diagonal matrix $\boldsymbol{D} = \mathrm{diag}(s_{u2}, s_{\omega 2}, \ldots, s_{un}, s_{\omega n}) \in \mathbb{R}^{2(n-1)\times 2(n-1)}$. Then, stacking the preceding equations for all followers, we obtain

$$\begin{aligned}\dot{\boldsymbol{h}}_F &= \boldsymbol{D}\Big[-k_P[\boldsymbol{L}_{fl}, \boldsymbol{L}_{ff}](\boldsymbol{h} - \boldsymbol{h}^*) - k_I \int_0^t [\boldsymbol{L}_{fl}, \boldsymbol{L}_{ff}](\boldsymbol{h} - \boldsymbol{h}^*)\mathrm{d}\tau\Big] \\ &= -k_P\boldsymbol{D}\Big[\boldsymbol{L}_{fl}\boldsymbol{h}_1 + \boldsymbol{L}_{ff}\boldsymbol{h}_F - [\boldsymbol{L}_{fl}, \boldsymbol{L}_{ff}]\boldsymbol{h}^*\Big] - k_I\boldsymbol{D}\int_0^t [\boldsymbol{L}_{fl}, \boldsymbol{L}_{ff}](\boldsymbol{h} - \boldsymbol{h}^*)\mathrm{d}\tau \\ &\overset{(6)}{=} -k_P\boldsymbol{D}\boldsymbol{L}_{ff}(\boldsymbol{h}_F - \boldsymbol{h}_F^*) - k_I\boldsymbol{D}\int_0^t [\boldsymbol{L}_{fl}, \boldsymbol{L}_{ff}](\boldsymbol{h}(\tau) - \boldsymbol{h}^*(\tau))\mathrm{d}\tau.\end{aligned}$$

Define $\boldsymbol{\zeta}_F = \int_0^t [\boldsymbol{L}_{fl}, \boldsymbol{L}_{ff}](\boldsymbol{h}(\tau) - \boldsymbol{h}^*(\tau))\mathrm{d}\tau$ and thus

$$\dot{\boldsymbol{\zeta}}_F = \boldsymbol{L}_{ff}(\boldsymbol{h}_F - \boldsymbol{h}_F^*) = \boldsymbol{L}_{ff}\boldsymbol{\delta}_F. \tag{10}$$

Consequently, from the preceding relationships, we obtain the following linear time-varying system

$$\begin{bmatrix} \dot{\boldsymbol{\delta}}_F \\ \dot{\boldsymbol{\zeta}}_F \end{bmatrix} = \begin{bmatrix} -k_P\boldsymbol{D}\boldsymbol{L}_{ff} & -k_I\boldsymbol{D} \\ \boldsymbol{L}_{ff} & \boldsymbol{0} \end{bmatrix} \begin{bmatrix} \boldsymbol{\delta}_F \\ \boldsymbol{\zeta}_F - \boldsymbol{L}_{ff}^{-1}\boldsymbol{L}_{fl}\boldsymbol{v}_c/k_I \end{bmatrix}, \tag{11}$$

where $\boldsymbol{v}_c \in \mathbb{R}^2$ is the piece-wise constant velocity of the leader. We can now prove the convergence of the system to the target formation.

Theorem 1. *Let Assumption 1 hold. Under the action of tracking control law (9) under input saturation, the follower robots converge to the target formation asymptotically, i.e., $\boldsymbol{\delta}_F = \boldsymbol{h}_F - \boldsymbol{h}_F^* \to \boldsymbol{0}$ as $t \to \infty$.*

Proof. Note that the structure of $\boldsymbol{D}\boldsymbol{L}_{ff}$ is a weighted version of $\boldsymbol{L}_{ff}$ with positive weights s_{ui} and $s_{\omega i} \in (0, 1]$. More specifically, the (i, j)-th block matrix of $\boldsymbol{D}\boldsymbol{L}_{ff}$ is $\begin{bmatrix} -s_{ui}l_{ij} & 0 \\ 0 & -s_{\omega i}l_{ij} \end{bmatrix}$ and the

block matrix on the diagonals is $\begin{bmatrix} s_{ui}|\mathcal{N}_i| & 0 \\ 0 & s_{\omega i}|\mathcal{N}_i| \end{bmatrix}$, where $|\mathcal{N}_i|$ is the number of neighboring robots of robot i. Thus, $\boldsymbol{DL}_{ff}$ corresponds to the follower part of the Lalacian matrix of the weighted graph of $\mathcal{G}$ and hence has eigenvalues with positive real parts.

The characteristic equation of the (time-varying) state matrix in (11) is given by the Schur's formula as

$$\begin{aligned}\det(\lambda \boldsymbol{I}_{2(n-1)})\det(\lambda \boldsymbol{I}_{2(n-1)} + k_P \boldsymbol{DL}_{ff} + k_I \lambda^{-1} \boldsymbol{DL}_{ff}) \\ = \det(\lambda^2 \boldsymbol{I}_{2(n-1)} + \lambda k_P \boldsymbol{DL}_{ff} + k_I \boldsymbol{DL}_{ff}).\end{aligned}$$

Denote $\mu_i, i = 1, \ldots, 2(n-1)$, as the eigenvalues of $\boldsymbol{DL}_{ff}$, which have positive real parts. Then λ are the solutions to $\lambda^2 + k_P \mu_i \lambda + k_I \mu_i$, $i = 1, \ldots, 2(n-1)$. Thus, $\lambda = -k_P \mu_i \pm \sqrt{k_P^2 \mu_i^2 - 4 k_I \mu_i}/2, i = 1, \ldots, 2(n-1)$, which have negative real parts. As a consequence, the state matrix in (11) is a Hurwitz matrix uniformly. Therefore, $\boldsymbol{\delta}_F \to \boldsymbol{0}$ and $\boldsymbol{\zeta}_F \to \boldsymbol{L}_{ff}^{-1} \boldsymbol{L}_{fl} \boldsymbol{v}_c / k_I$ asymptotically as $t \to \infty$. □

4. SIMULATION

This section provides the simulation results of formation tracking of six mobile agents in two dimensions in Fig. 2.

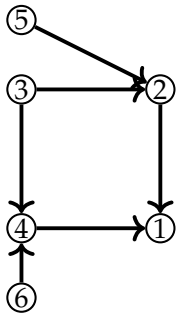

(a) The interaction graph $\mathcal{G}$

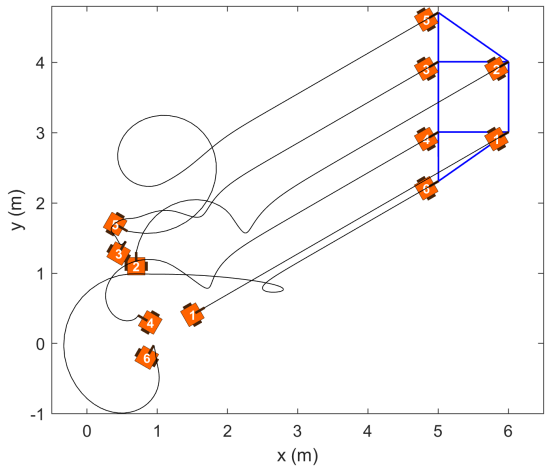

(b) Trajectories of the robots (gray solid lines)

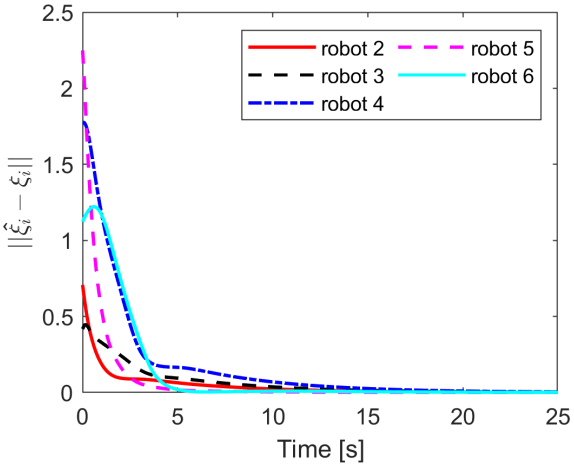

(c) Heading estimation errors versus time

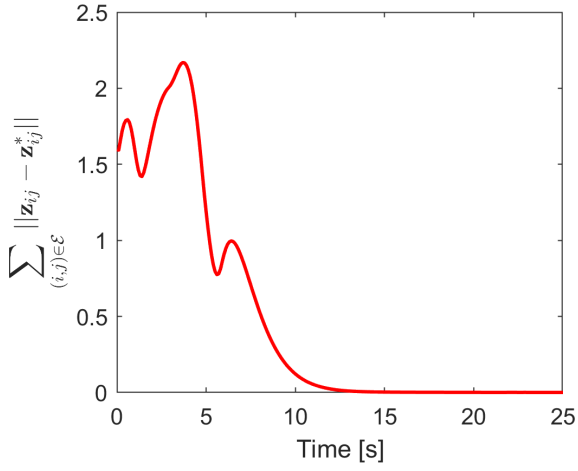

(d) Formation control error versus time

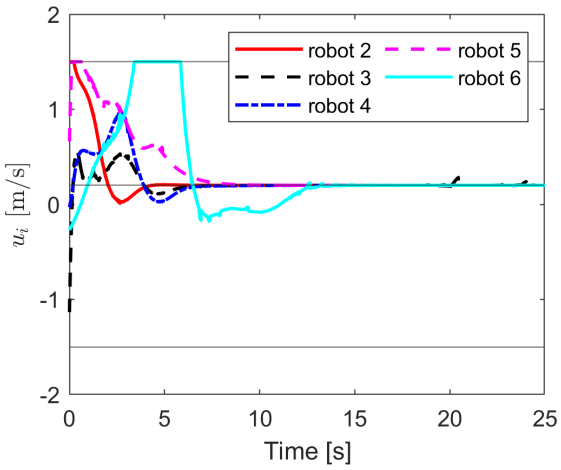

(e) Heading speeds u_i versus time

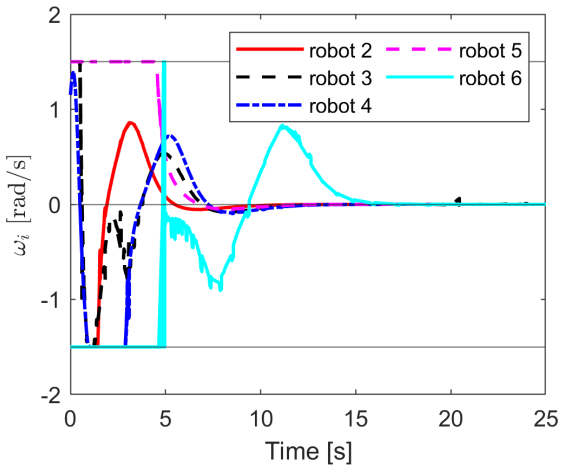

(f) Angular velocities ω_i versus time

Fig. 2. Simulation results of formation tracking of six mobile robots under the controller (9)

The graph of the robots in Fig. 2(a) contains a spanning tree rooted at the leader 1, thus satisfying Assumption 1. The leader moves at a constant speed $u_1 = 0.2$ m/s and a heading angle of $\theta_1 = \pi/6$ rad. The initial positions and desired formation (blue lines) of the system are given in Fig. 2(b). The initial heading angles of the followers are $\theta_2 = \pi/2, \theta_3 = \pi/3, \theta_4 = 4\pi/6, \theta_5 = -\pi/6$, and $\theta_6 = \pi/3$ rad. The control gains are $k_P = 2$ and $k_I = 1$, and the control points' offset is $L_i = 0.2$ m. The velocities of the robots are saturated by $-1.5 \geq u_i \leq 1.5$ m/s and $-1.5 \geq \omega_i \leq 1.5$ rad/s, as shown in Figs. 2(e) and 2(f), respectively. Fig. 2(c) shows that the heading vectors of the robots can be estimated by (3) asymptotically as time increases. The robot system achieves the target formation (the blue lines in Fig. 2(b)) as the total control error $\sum_{(i,j)\in\mathcal{E}} \|z_{ij} - z_{ij^*}\| \to 0$ as time diverges (Fig. 2(d)). The heading speeds of the follower robots converge to that of the leader, i.e., $u_1 = 0.2$ m/s, as depicted in Fig. 2(e).

5. EXPERIMENT

We provide experimental results on the formation tracking of a system consisting of two follower Turtlebot3 mobile robots (Fig. 3(a)) and a virtual leader. A video of the experiment can be seen at https://youtu.be/aKNtx02GNHQ. The parameters of a Turtlebot3 are given in Table 1.

Table 1. Parameters of a Turtlebot3 Burger

Maximum translational velocity	$\pm$0.22 m/s
Maximum rotational velocity	2.84 rad/s
Dimensions	138mm x 178mm x 192mm
Weight	1 kg
Board Computer	Raspberry Pi 4
MCU	32-bit ARM Cortex®-M7
Actuator	XL430-W250
Laser Distance Sensor	360 Laser Sensor LDS-02
IMU	Gyroscope 3 Axis, Accelerometer 3 Axis

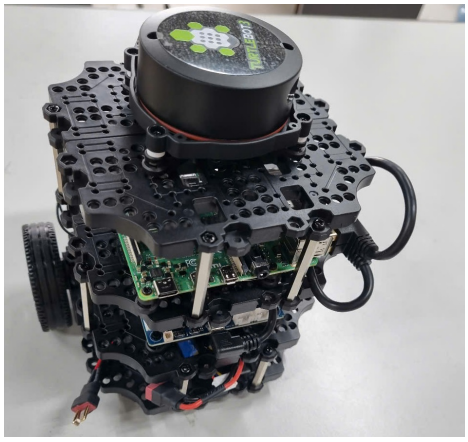

(a) Turtle3 Burger mobile robot

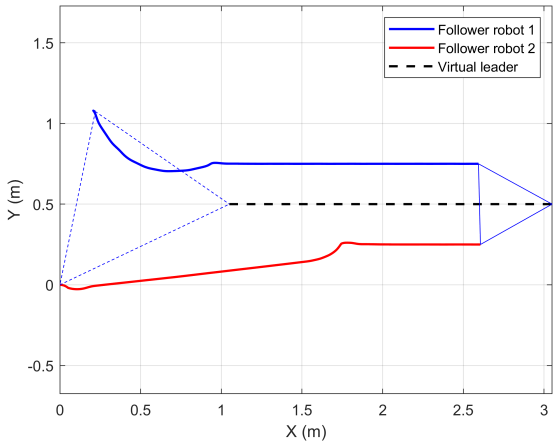

(b) Trajectories of the follower robots (solid lines)

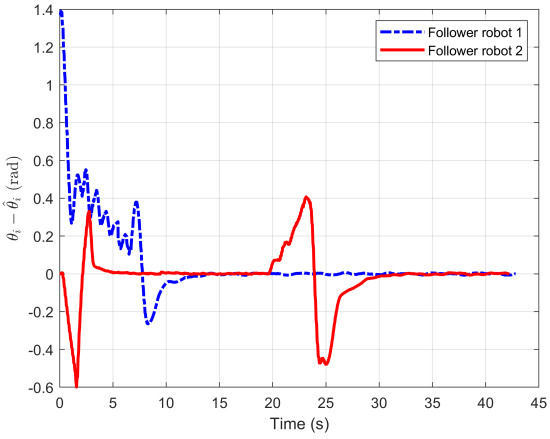

(c) Heading angle errors versus time

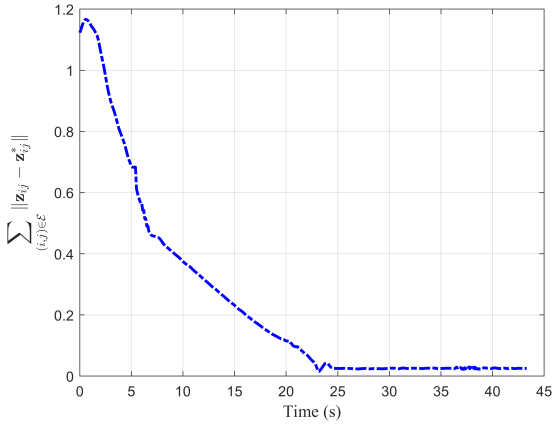

(d) Formation control error versus time

Fig. 3. Orientation estimation error (top) and formation control error (below) versus time

The control project was coded using open source ROS 2 in Ubuntu 22.04.5. In ROS 2, each Turtlebot3 robot when operated is assigned a unique namespace (*/robot1*, */robot2*, ...) to avoid topic conflicts. Consequently, the active topics are structured with a prefix, e.g., */robot1/cmd_vel* and */robot2/cmd_vel* (Fig. 4).

To obtain the position, each Turtlebot3 robot publishes odometry data on the /odom topic (in *nav_msgs/msg/Odometry*) and receives control inputs through the /cmd_vel topic (in *geometry_msgs/msg/Twist*). A central node (i.e., control_node), running on a PC, subscribes to the /odom topics of the follower robots, processes the data, and computes the command linear and angular velocities (u_i, r_i) according to controller (9). These velocity commands are then published back to the respective /cmd_vel topics of each robot.

In the experiment, the leader was a virtual robot that moved with a constant speed $u_l = 0.05$ m/s and a zero heading angle. Its position is thus easily updated with time in the computer program, i.e., $x_l = x_l(0) + 0.05t$ and $y_l = y_l(0)$ m. Two follower Turtlebot3s, 1 and 2, had directed links to the leader; their relative positions to the virtual leader were computed. The desired formation shape is an equilateral triangle with a side length of 0.5 m. The control gains in (9) were chosen as $k_P = 2, k_I = 0.2$, and $L_i = 0.05$ m. As can be observed from Fig. 3(c), the heading angles of robots 1 and 2 were estimated from their respective global position coordinates. The robot system was steered to the target formation (blue triangle in Fig. 3(b)) asymptotically as the control error converged to near zero as shown in Fig. 3(d).

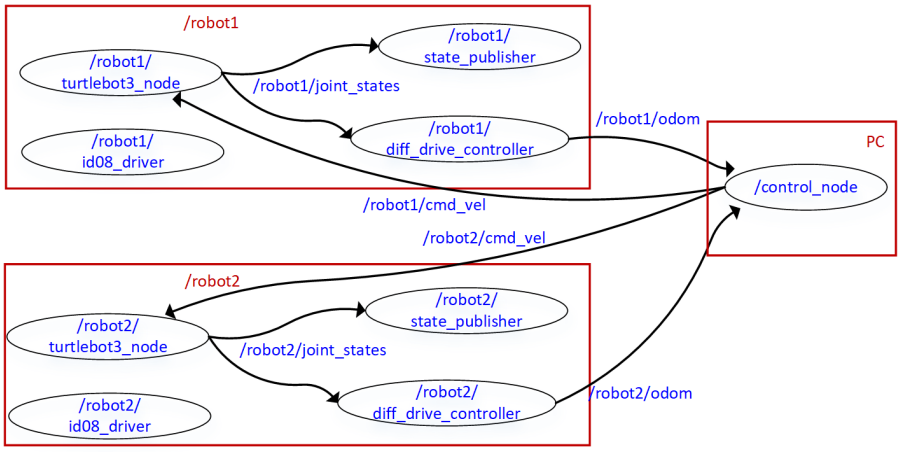

Fig. 4. ROS 2 topics graph of two TurtleBot3 robots with distinct namespaces. The control_node subscribes to odometry data and publishes velocity commands to each robot via wireless communication

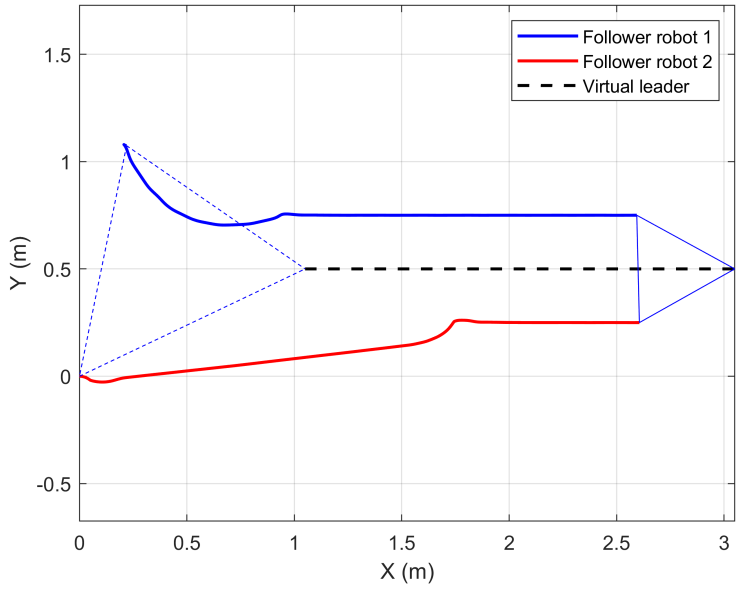

Fig. 5. The trajectories of the robots in the experiment

6. CONCLUSION

In this work, we investigated the formation tracking of a fleet of multiple wheeled ground mobile robots subject to velocity input limits. The target formation of the robots involves the rectilinear motion of the leader with a constant speed and the followers' maintenance of the relative positions between certain control points and neighboring robots. The sensing of relative positions in local coordinates is characterized by a directed graph that contains a spanning tree rooted at the leader. The heading angles of the robots were estimated from the global coordinates of their respective centers. The tracking controllers for the follower robots were devised based on the heading estimates and the relative positions between neighboring robots in the followers' local coordinates. The formation has been shown to converge to the target formation asymptotically. Simulation and experimental results were provided to support the theoretical analysis.

The impact of velocity saturation on the convergence rate of the target formation will be addressed in future work.

DECLARATION OF COMPETING INTEREST

The authors declare that they have no known competing financial interests or personal relationships that could have appeared to influence the work reported in this paper.

CREDIT AUTHOR STATEMENT

Quoc Van Tran: *Conceptualization, Methodology, Validation, Resources, Formal analysis, Visualization, Writing – original draft, Writing – review & editing, Supervision, Funding acquisition*. Ngoc-Bao Huu Tran: *Conceptualization, Software, Investigation, Writing – original draft*. Quang-Hoang Nguyen: *Conceptualization, Validation, Writing – review & editing*.

FUNDING

This research received no specific grant from any funding agency in the public, commercial, or not-for-profit sectors.

REFERENCES

Ahn, H.-S. (2019). *Formation control: Approaches for distributed agents*. Springer International Publishing. https://doi.org/10.1007/978-3-030-15187-4

Cao, D. S., & Tran, Q. V. (2025). Adaptive path-following control of underactuated surface vessels subject to unknown disturbances with uniform bounded lateral motion. *International Journal of Control, Automation and Systems*, *23*(6), 1641–1651. https://doi.org/10.1007/s12555-024-0916-y

Chen, J., Jayawardhana, B., & de Marina, H. G. (2024). Distributed distance-based formation-motion control of unicycle agents without orientation measurements. *IEEE Transactions on Control of Network Systems*, 1–8. https://doi.org/10.1109/TCNS.2024.3435148

Chen, L., de Marina, H. G., & Cao, M. (2022). Maneuvering formations of mobile agents using designed mismatched angles. *IEEE Transactions on Automatic Control*, *67*(4), 1655–1668. https://doi.org/10.1109/TAC.2021.3066388

Chen, L., Xiao, J., Lin, R. C. H., & Feroskhan, M. (2023). Angle-constrained formation maneuvering of unmanned aerial vehicles. *IEEE Transactions on Control Systems Technology*, *31*(4), 1733–1746. https://doi.org/10.1109/TCST.2023.3240286

Do, K. D. (2008). Formation tracking control of unicycle-type mobile robots with limited sensing ranges. *IEEE Transactions on Control Systems Technology*, *16*(3), 527–538. https://doi.org/10.1109/TCST.2007.908214

Khaledyan, M., Liu, T., Fernandez-Kim, V., & de Queiroz, M. (2020). Flocking and target interception control for formations of nonholonomic kinematic agents. *IEEE Transactions on Control Systems Technology*, *28*(4), 1603–1610. https://doi.org/10.1109/TCST.2019.2914994

Kwon, S.-H., Sun, Z., Anderson, B. D. O., & Ahn, H.-S. (2022). Sign rigidity theory and application to formation specification control. *Automatica*, *141*, 110291. https://doi.org/https://doi.org/10.1016/j.automatica.2022.110291

Li, X., Wen, C., Fang, X., & Wang, J. (2022). Adaptive bearing-only formation tracking control for nonholonomic multiagent systems. *IEEE Transactions on Cybernetics*, *52*(8), 7552–7562. https://doi.org/10.1109/TCYB.2020.3042491

Lu, K., Dai, S.-L., & Jin, X. (2024). Fixed-time rigidity-based formation maneuvering for nonholonomic multirobot systems with prescribed performance. *IEEE Transactions on Cybernetics*, *54*(4), 2129–2141. https://doi.org/10.1109/TCYB.2022.3226297

Maghenem, M., Loría, A., & Panteley, E. (2018). A cascades approach to formation-tracking stabilization of force-controlled autonomous vehicles. *IEEE Transactions on Automatic Control*, *63*(8), 2662–2669. https://doi.org/10.1109/TAC.2017.2774003

Schuck, M., Dahanaggamaarachchi, D. O., Sprenger, B., Vyas, V., Zhou, S., & Schoellig, A. P. (2025). SwarmGPT: Combining large language models with safe motion planning for drone swarm choreography. *IEEE Robotics and Automation Letters*. https://doi.org/10.1109/LRA.2025.3619745

Sun, G., Zhou, R., Ma, Z., Li, Y., Groß, R., Chen, Z., & Zhao, S. (2023). Mean-shift exploration in shape assembly of robot swarms. *Nature Communications*, *14*(3476). https://doi.org/10.1038/s41467-023-39251-5

Sun, Z., de Marina, H. G., Seyboth, G. S., Anderson, B. D. O., & Yu, C. (2019). Circular formation control of multiple unicycle-type agents with nonidentical constant speeds. *IEEE Transactions on Control Systems Technology*, *27*(1), 192–205. https://doi.org/10.1109/TCST.2017.2763938

Tran, Q. V., & Ahn, H.-S. (2020). Distributed formation control of mobile agents via global orientation estimation. *IEEE Transactions on Control of Network Systems*, *4*(7), 1654–1664. https://doi.org/10.1109/tcns.2020.2993253

Tran, Q. V., Do, D.-K., & Pham, T.-T. (2025). Formation maneuver of wheeled mobile robots based on attitude estimation. *Proceedings of the Fourth International Conference on Material, Machines, and Methods for Sustainable Development*, 1–7. https://doi.org/10.1007/978-3-031-96126-7_1

Tran, Q. V., & Kim, J. (Mar. 2022). Bearing-constrained formation tracking control of nonholonomic agents without inter-agent communication. *IEEE Control Systems Letters*, *6*, 2401–2406. https://doi.org/10.1109/LCSYS.2022.3159128

Tran, Q. V., Lee, C., Kim, J., & Nguyen, H. Q. (2023). Robust bearing-based formation tracking control of underactuated surface vessels: An output regulation approach. *IEEE Transactions on Control of Network Systems*, *10*(4), 2048–2059. https://doi.org/10.1109/TCNS.2023.3259105

Vu, H. M., Trinh, M. H., Van Tran, Q., & Ahn, H.-S. (2024). Distance-based formation tracking of single- and double-integrator agents. *IEEE Transactions on Automatic Control*, *69*(2), 1332–1339. https://doi.org/10.1109/TAC.2023.3299817

Yan, L., Ma, B., Jia, Y., & Jia, Y. (2024). Observer-based trajectory tracking control of nonholonomic wheeled mobile robots. *IEEE Transactions on Control Systems Technology*, *32*(3), 1114–1121. https://doi.org/10.1109/tcst.2024.3351073

Zhao, S., & Zelazo, D. (2015). Bearing rigidity and almost global bearing-only formation stabilization. *IEEE Transactions on Automatic Control*, *61*(5), 1255–1268. https://doi.org/10.1109/tac.2015.2459191